University of Montana

ScholarWorks at University of Montana

Numerical Terradynamic Simulation Group Publications

Numerical Terradynamic Simulation Group

2006

Spring Thaw and Its Effect on Terrestrial Vegetation Productivity in the Western Arctic Observed from Satellite Microwave and Optical Remote Sensing

John S. Kimball
University of Montana - Missoula

K. C. McDonald

M. Zhao

Follow this and additional works at: https://scholarworks.umt.edu/ntsg_pubs

Let us know how access to this document benefits you.

Recommended Citation

Spring Thaw and Its Effect on Terrestrial Vegetation Productivity in the Western Arctic Observed from Satellite Microwave and Optical Remote Sensing

J. S. Kimball*

Flathead Lake Biological Station, University of Montana, Polson, Montana

K. C. McDonald

Jet Propulsion Laboratory, California Institute of Technology, Pasadena, California

M. Zhao

Numerical Terradynamic Simulation Group, College of Forestry and Conservation, University of Montana, Missoula, Montana

ABSTRACT: Global satellite remote sensing records show evidence of recent vegetation greening and an advancing growing season at high latitudes. Satellite remote sensing–derived measures of photosynthetic leaf area index (LAI) and vegetation gross and net primary productivity (GPP and NPP) from the NOAA Advanced Very High Resolution Radiometer (AVHRR) Pathfinder

* Corresponding author address: J. S. Kimball, Flathead Lake Biological Station, University of Montana, 311 Biostation Lane, Polson, MT 59860-9659.

E-mail address: johnk@ntsg.umt.edu

record are utilized to assess annual variability in vegetation productivity for Alaska and northwest Canada in association with the Western Arctic Linkage Experiment (WALE). These results are compared with satellite microwave remote sensing measurements of springtime thaw from the Special Sensor Microwave Imager (SSM/I). The SSM/I-derived timing of the primary spring-time thaw event was well correlated with annual anomalies in maximum LAI in spring and summer ($P \leq 0.009$; $n = 13$), and GPP and NPP ($P \leq 0.0002$) for the region. Mean annual variability in springtime thaw was on the order of ±7 days, with corresponding impacts to annual productivity of approximately 1% day^{-1}. Years with relatively early seasonal thawing showed generally greater LAI and annual productivity, while years with delayed seasonal thaw-ing showed corresponding reductions in canopy cover and productivity. The apparent sensitivity of LAI and vegetation productivity to springtime thaw indicates that a recent advance in the seasonal thaw cycle and associated lengthening of the potential period of photosynthesis in spring is sufficient to account for the sign and magnitude of an estimated positive vegetation pro-ductivity trend for the western Arctic from 1982 to 2000.

KEYWORDS: AVHRR; Boreal; Arctic; Carbon; NPP; GPP; LAI; Phenol-ogy; Freeze–thaw; SSM/I; WALE

1. Introduction

Each spring approximately 50 million km^2 of Earth's terrestrial Northern Hemi-sphere undergoes a seasonal transition from predominantly frozen to nonfrozen (i.e., thawed) conditions (Robinson et al. 1993). These relatively abrupt seasonal transitions represent the closest analog to a biospheric on/off switch existing in nature, affecting surface meteorological conditions, ecological trace gas dynamics, energy exchange, and hydrologic activity profoundly. Net primary production (NPP) is the primary conduit of carbon transfer from the atmosphere to the land surface and is thus a fundamental component of the global carbon cycle. In seasonally frozen environments, vegetation productivity is constrained by low temperatures and plant-available moisture for much of the year, while the active growing season is primarily determined by length of the nonfrozen period (Jarvis and Linder 2000; Kimball et al. 2004).

Boreal forest and arctic tundra biomes of the northern high (>50°N) latitudes are undergoing significant change coinciding with recent and persistent climatic warming for the region (Serreze et al. 2000; Comiso 2003). Satellite records and regional modeling studies indicate a recent advance in spring thaw and growing season onset for the northern high latitudes (McDonald et al. 2004; Smith et al. 2004; Euskirchen et al. 2006). The growing season advance coincides with both earlier and larger drawdown of atmospheric CO$_2$ (Keeling et al. 1996; McDonald et al. 2004) and summer greening (Myneni et al. 1997a), indicating a generally positive boreal-arctic NPP response. However, other studies indicate a more vari-able productivity response to regional warming and associated earlier and longer growing seasons depending on soil moisture and nutrient availability, vegetation type, and disturbance regime (Barber et al. 2000; Kimball et al. 2000; Wilmking et al. 2004; Goetz et al. 2005).

The Western Arctic Linkage Experiment (WALE) was initiated to investigate

the role of northern terrestrial ecosystems in the larger Arctic system response to global change through model and satellite remote sensing analyses of regional carbon, water, and energy cycles (McGuire et al. 2006). A companion WALE analysis of regional productivity trends for Alaska and northwest Canada showed a moderate, but widespread, positive trend in vegetation productivity from 1982 to 2000 coinciding with summer warming and subsequent relaxation of cold temperature constraints to plant growth (Kimball et al. 2006). The objective of the current investigation is to clarify the role of spring thaw timing in determining annual vegetation productivity, and whether a recent advance in the northern seasonal thaw cycle is sufficient to account for the sign and magnitude of the estimated positive vegetation productivity trend for the western Arctic. To accomplish this objective we conducted a temporal change classification of daily terrestrial microwave emissions from the SSM/I time series to determine the spatial pattern and annual variability of the primary springtime thaw event for Alaska and northwest Canada from 1988 to 2000. We also applied a biome-specific production efficiency model (PEM) driven by daily surface meteorological inputs from the National Centers for Environmental Prediction–National Center for Atmospheric Research (NCEP–NCAR) reanalysis (Kistler et al. 2001) and National Oceanic and Atmospheric Administration (NOAA) Advanced Very High Resolution Radiometer (AVHRR) Pathfinder monthly time series observations of photosynthetic leaf area and canopy absorbed solar radiation to assess spatial patterns and annual variability in vegetation structure and productivity for the region. We evaluated the statistical correspondence between these variables and seasonal weather patterns for the domain, and the degree to which the onset of the growing season, inferred from the SSM/I record, determines annual variability in regional vegetation productivity indicated by the AVHRR Pathfinder record and PEM results.

2. Methods

The WALE domain encompasses boreal forest and arctic tundra biomes of Alaska and northwest Canada (Figure 1). The region is defined in terms of nodes of the National Snow and Ice Data Center (NSIDC) north polar Equal-Area Scalable Earth (EASE) Grid (Armstrong and Brodzik 1995). The study domain spans a latitudinal range from $56.19°$ to $71.24°$N, while land areas within the region comprise 3511 grid cells with nominal 25 km × 25 km resolution and a total representative area of approximately 2.2 million km^2. We used a NOAA AVHRR–based global land cover classification to define major biomes for PEM calculations within the study region (Myneni et al. 1997b; DeFries et al. 1998). Boreal forests and tundra are the major biomes within the region and represent approximately 52% and 30% of the region, respectively. The rest of the domain is composed of permanent ice and snow, barren land, and inland water bodies. These nonvegetated areas were masked from further analysis to isolate relationships between PEM results and environmental parameters.

2.1. Production efficiency model calculations

A biome-specific PEM was used to calculate gross primary productivity (GPP) and NPP for unmasked pixels within the 25-km resolution EASE-Grid domain.
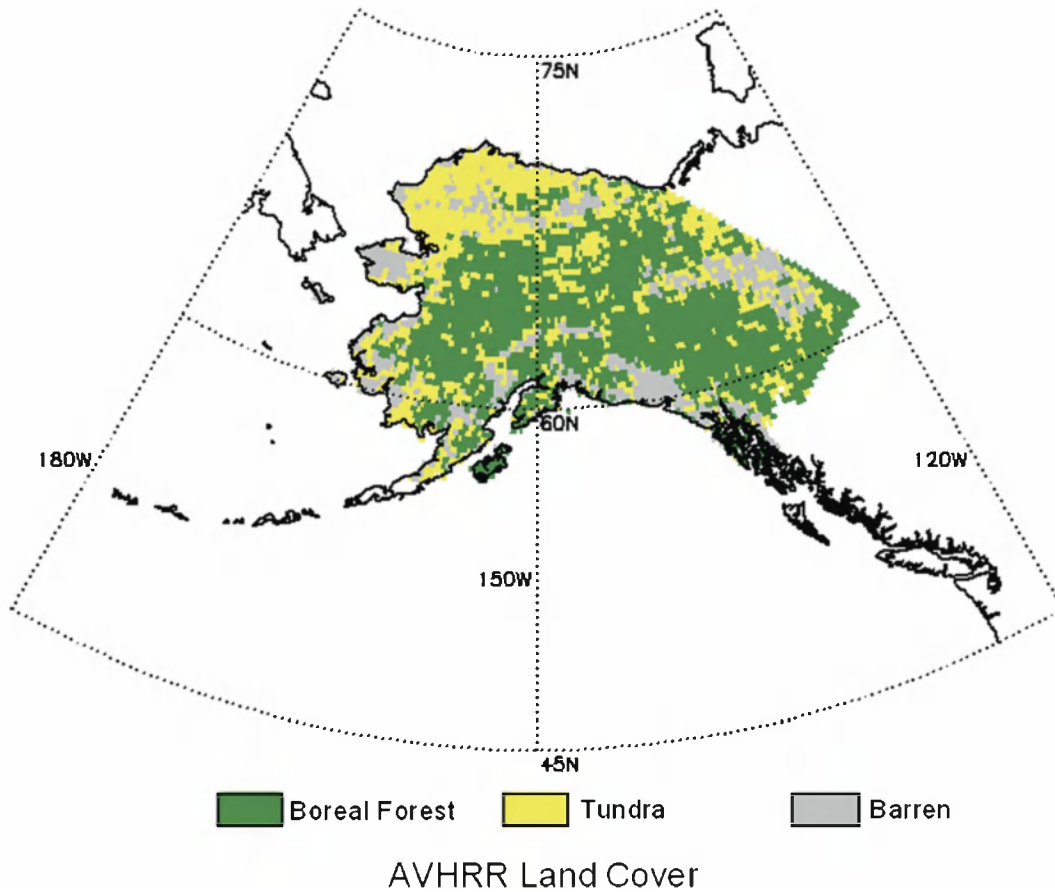
Figure 1. The WALE study domain spans a latitudinal range from 56.19° to 71.24°N, with a total representative area of approximately 2.2 million km^2; boreal forest and arctic tundra biomes represent 52% and 30% of the domain, while areas in gray represent permanent ice and snow, barren land, and inland water bodies that were not included in this analysis.

The PEM logic is described and verified in detail elsewhere (e.g., Running et al. 2000; Zhao et al. 2005; Heinsch et al. 2006) and summarized below. Gross primary production (g C m^{-2}) was derived on a daily basis as

$$GPP = \varepsilon \times FPAR \times PAR \tag{1}$$

$$\varepsilon = \varepsilon_{max} \times T_f \times VPD_f, \tag{2}$$

where ε is a light use efficiency parameter (g C MJ^{-1}) for the conversion of photosynthetically active radiation (PAR; MJ m^{-2}) to GPP, where PAR is assumed to represent 45% of incident solar radiation; FPAR is the fraction of absorbed PAR; ε_{max} is the potential maximum ε under optimal conditions (i.e., no environmental stress); T_f is a scalar that defines reductions in photosynthesis under low temperature conditions; and VPD$_f$ is a scalar that defines similar reductions under suboptimal surface air vapor pressure deficit (VPD) and associated daytime water

stress conditions. Both T_f and VPD_f are dimensionless parameters ranging from 1 for optimal conditions to 0 under complete canopy stomatal closure and minimal photosynthetic activity. Both T_f and VPD_f are defined from daily air temperature (T_{min}) and VPD using simple photosynthetic response curves. These response curves and $\varepsilon_{\mathrm{max}}$ are prescribed for different biome types defined from the global land cover classification.

Net primary production (g C m^{-2}) is derived on an annual basis as the difference between the annual summation of daily net photosynthesis and autotrophic growth and maintenance respiration:

$$\mathrm{NPP} = \sum_{1}^{365} (\mathrm{GPP} - R_{m\_lr}) - (R_{m\_w} + R_g), \tag{3}$$

where R_{m_lr} is the daily maintenance respiration of leaves and fine roots as derived from allometric relationships to canopy leaf area index (LAI) and an exponential relationship between respiration and temperature. The R_{m_w} parameter represents the annual maintenance respiration from live wood, while R_g represents annual growth respiration; both R_{m_w} and R_g are derived from allometric relationships between vegetation biomass and maximum annual LAI and exponential respiration response curves to air temperature. The characteristic response curves for these calculations vary according to major biomes as defined by a Biome Properties Lookup Table (BPLUT) and the global land cover classification. The BPLUT defines response characteristics for 11 major biomes including evergreen and deciduous needleleaf and broadleaf forests, mixed deciduous and evergreen forests, grasslands, shrublands, and croplands. The PEM used for this investigation is currently being used for operational global assessment and monitoring of GPP and NPP using LAI and FPAR data from the Moderate Resolution Imagine Spectroradiometer (MODIS) sensor onboard the National Aeronautics and Space Administration (NASA) Earth Observing System (EOS) *Terra* satellite from 2000 onward (Running et al. 2004; Zhao et al. 2005). A detailed description of these algorithms and associated BPLUT properties can be found in the MODIS MOD17 User's Guide (Heinsch et al. 2003).

For this investigation, we applied the PEM described above to assess spatial and temporal variability in annual vegetation productivity for the study region over a 13-yr period from 1988 to 2000. The PEM requires spatially explicit and temporally contiguous inputs of daily surface meteorology, and daily LAI and FPAR information, to compute GPP and NPP. Monthly LAI and FPAR data were obtained from the NOAA AVHRR Pathfinder dataset, which has an approximate 16-km spatial resolution and extends over the entire domain from 1982 to 2000 (James and Kalluri 1994; Myneni et al. 1997b). The LAI and FPAR data are based on a monthly maximum value compositing of AVHRR spectral reflectance data to mitigate cloud cover, smoke, and other atmospheric aerosol contamination effects (Myneni et al. 1997b). These data were reprojected to the 25-km polar EASE-Grid format using a nearest-neighbor resampling scheme. The monthly LAI and FPAR data were then resampled to a daily time step by temporal linear interpolation of adjacent monthly values. The daily linear interpolation approach used for this investigation is a relatively simple but effective means for producing a daily FPAR and LAI time series for PEM simulations and has been used extensively for global

vegetation analyses of the AVHRR Pathfinder series (Myneni et al. 1997b; Nemani et al. 2003). Surface air temperature, incident solar radiation, and VPD inputs were provided by daily reanalysis data from NCEP (Kistler et al. 2001; Drobot et al. 2006). The NCEP meteorological data are available globally in approximately 1.875° (~208 km) spatial resolution and were reprojected into the 25-km resolution polar EASE-Grid format using a bi-Lagrangian interpolation approach (Serreze et al. 2002). PEM calculations were conducted for vegetated cells within the study region from 1988 to 2000, and spatial patterns and annual variability in GPP and NPP were evaluated accordingly.

To isolate the relative contributions of meteorological and vegetation structural parameters to the observed temporal response of GPP and NPP calculations, we conducted a series of PEM simulations over the 1988 to 2000 period by 1) constraining daily meteorological inputs to constant (1982) conditions while allowing model LAI and FPAR inputs to vary; and 2) constraining LAI and FPAR inputs to constant conditions while allowing daily meteorological inputs to vary. We then conducted a statistical correlation analysis of these results relative to PEM calculations derived from historical variability in both meteorological and LAI and FPAR time series inputs. These simulations provided a mechanism for isolating climate impacts to vegetation productivity from other potential impacts such as atmospheric nitrogen and CO_2 fertilization, disturbance, and forest succession; and from residual sensor calibration and aerosol effects on LAI and FPAR data.

2.2. Classification of primary seasonal thaw events

The Special Sensor Microwave Imager (SSM/I) is a multifrequency, linearly polarized passive microwave radiometer operating with a constant incidence angle of 53.1° and has flown on the Defense Meteorological Satellite Program (DMSP) platform series. Coverage is global and began in August 1987. We utilized the 19-GHz horizontally polarized channel, which has a native 70 km × 45 km footprint resolution. Data for this study were acquired as globally gridded brightness temperatures derived from orbital (swath) data (Armstrong et al. 2002). The SSM/I sensors have 6 A.M. and 6 P.M. equatorial crossing times for ascending or descending orbital nodes, where crossing time and respective nodes vary within the DMSP series. Brightness temperature data corresponding to orbital passes with 6 P.M. equatorial crossing times were mapped to the 25-km resolution polar EASE-Grid for each 24-h period and used for temporal classification of primary thaw events. The data gridding scheme maximizes the radiometric integrity of the original brightness temperature values, maintains high spatial and temporal precision, and involves no averaging of original swath data. Daily SSM/I data, spanning winter 1988 through winter 2000, were assembled onto the 25-km EASE-Grid covering the study domain. The daily composite data allow examination of annual thaw cycles from 1988 to 2000.

A material's radiometric brightness temperature T_B is characterized by its emissivity e, as $T_B = e\,T$, where T is its physical temperature (K). Emissivity is a unitless variable ranging from 0 for a perfectly nonemitting material to 1 for a perfect emitter (blackbody) (Ulaby et al. 1986). Emissivity is a function of the material's dielectric constant and is directly sensitive to the phase (solid/liquid) of water within the media. As water changes from a solid to a liquid phase, its

dielectric constant increases dramatically and significant increases in e and T_B result. Defining freeze/thaw as the predominant state (solid or liquid) of water within the landscape, we utilize the temporal change in T_B associated with the primary landscape springtime thaw event to monitor the timing of thaw across the study domain.

Previous studies have employed thresholding schemes based on time series signal processing to examine springtime thaw transitions with high temporal repeat satellite radar remote sensing data (Frolking et al. 1999; Kimball et al. 2001; Kimball et al. 2004). These algorithms characterize landscape thaw transition sequences utilizing the response of time series radar backscatter resulting from large changes in the bulk landscape dielectric constant occurring as the landscape thaws. As T_B responds similarly to the landscape dielectric constant, these approaches are also suitable for analysis of time series brightness temperature data.

We employed a step-edge detection scheme to identify the predominant springtime thaw transition event on an annual basis. In boreal regions, this event has been found to be generally coincident with the arrival of maximum surface wetness in spring associated with rising air temperatures, seasonal snowmelt, soil active layer thawing, and growing season onset (Kimball et al. 2004; McDonald et al. 2004). The technique is based on the application of an optimal edge detector for determining edge transitions in noisy signals (Canny 1986). The time of the primary springtime thaw event is determined from the convolution applied to T_B:

$$\mathrm{CNV}(t) = \int_{-\infty}^{\infty} f'(x)T_B(t-x)\,dx, \tag{4}$$

where $f'(x)$ is the first derivative of a normal (Gaussian) distribution. The occurrence of the primary springtime thaw event is then given by the time t_p when $\mathrm{CNV}(t)$ is a maximum. As the winter–spring transition progresses, the landscape may thaw and refreeze repeatedly. This technique accounts for the occurrence of weak edges, or less pronounced thaw events, as well as strong edges, and is less likely to classify minor thaw occurrences as the primary thaw event. This approach has been previously employed to examine thaw trends across the pan-Arctic basin and Alaska (McDonald et al. 2004). For this investigation, we apply a similar approach to map the primary spring thaw event on an annual basis for each 25-km grid cell within the study domain.

The thaw classification algorithm [Equation (4)] was applied to each annual time series of daily SSM/I brightness temperature data from 1988 to 2000, producing yearly maps of the primary spring thaw event across the study domain. Areas of permanent ice and snow, bare ground, and sparse vegetation cover were identified using the NOAA AVHRR–based global land cover classification (Myneni et al. 1997b; DeFries et al. 1998) and were masked from further analysis to isolate relationships between seasonal thawing and AVHRR-derived vegetation productivity.

2.3. Analysis

We applied the SSM/I and AVHRR Pathfinder time series using the methods above to determine regional patterns and temporal variability in spring thaw and

vegetation productivity for the WALE domain from 1988 to 2000. The remote sensing and associated model results were spatially aggregated across all unmasked grid cells in the study domain to produce regional averages of monthly, seasonal, and annual conditions. Temporal anomalies of springtime thaw, LAI, and PEM-derived GPP and NPP results were then calculated relative to long-term means or linear least squares regression results where significant ($P \leq 0.1$) secular trends were observed. We then conducted a statistical correlation analysis of the relationships between springtime thaw, LAI and annual productivity calculations, and mean NCEP surface meteorological parameters. The statistical significance of these relationships was assessed at the 90% confidence level.

3. Results

3.1. Spatial variability in spring thaw timing

A map of the average (1988–2000) timing of the primary springtime thaw event as derived from temporal classification of daily SSM/I brightness temperatures is presented in Figure 2 and summarized in Table 1. The springtime thaw event extends over a 12-week period from approximately 7 March (day 66) to 26 May (day 146), with generally earlier occurrence at lower latitudes and elevations. The spatial pattern of thawing also shows general distinctions among major land cover classes. Boreal forest and tundra areas show respective average thaw dates of approximately 12 April [day 102 ± 8.3 (s)] and 23 April [day 113 ± 5.6 (s)], with considerable overlap among regional biomes.

Previous studies have demonstrated that the satellite microwave remote sensing–derived timing of spring thaw coincides with the onset of seasonal snowmelt, soil thaw, and an associated rise in surface air temperatures in spring (Frolking et al. 1999; Kimball et al. 2001; Kimball et al. 2004; McDonald et al. 2004). The current results also show an inverse relationship between the SSM/I-derived timing of seasonal thawing and regional mean summer [June–August (JJA; hereafter 3-month periods are denoted by the first letter of each respective month)] air temperatures represented by the NCEP–NCAR reanalysis ($r = -0.701$; $P = 0.007$). Years with relatively early thawing coincide with warmer summers, while years with late seasonal thawing have generally cooler summers. There was no evidence of a significant relationship between thaw timing and mean annual air temperatures, however, or average seasonal temperatures in spring (MAM), winter (DJF), or fall (SON).

3.2. Relations between spring thaw timing and LAI

The average SSM/I-derived thaw date for the domain was 17 April [DOY 107 ± 6.67 days yr^{-1} (s)], while the AVHRR-derived onset of active canopy growth and maximum annual LAI occurred in April and July, respectively (see Figure 3). Annual variability in maximum monthly LAI was greatest during active canopy development in May [± 0.64 m^2 m^{-2} (s)], followed by the fall canopy senescence period [$0.32–0.55$ m^2 m^{-2} (s)]. The relatively large difference between summer and winter LAI is due to the effects of low solar illumination and lack of valid spectral reflectance data in winter at higher (>45°N) latitudes (Buermann et al.

Mean Primary Springtime Thaw Date
(1988-2000)
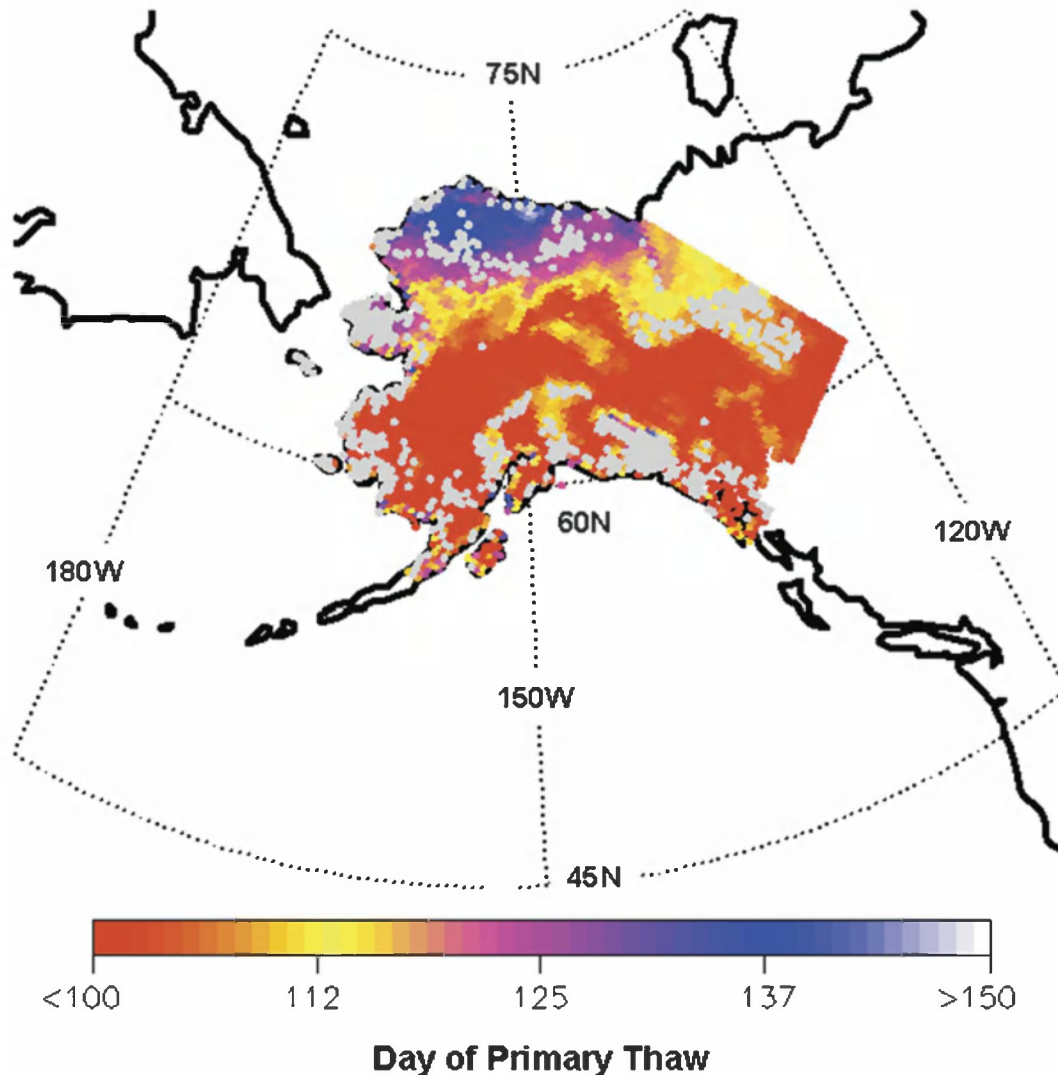

Day of Primary Thaw

Figure 2. Spatial pattern of the mean annual primary springtime thaw event for the 1988–2000 period as derived from temporal classification of daily, descending orbit (6 P.M. local overpass), 19-GHz brightness temperature data from the SSM/I sensor series. Barren land and other nonvegetated surfaces were excluded from the analysis and are shown in gray, while areas outside the study region are shown in white.

2001). Year-to-year variability in maximum annual LAI represented 2.4% [i.e., ± 0.13 m^2 m^{-2} (s)] of mean maximum canopy conditions for the domain and was small relative to temperate deciduous forests and grasslands because of the greater leaf longevity of evergreen-dominated boreal ecosystems (Viereck and Little

Table 1. Summary of GPP, NPP, and primary thaw event results for the vegetated study domain.

| Classification region	Area[a] (%)	GPP[b] (g C m^{-2} yr^{-1})	NPP[b] (g C m^{-2} yr^{-1})	Thaw date[c] (DOY)
Entire domain	100.0	596.6 (173.7)	301.2 (107.4)	106 (20)
Boreal forest	52.0	672.7 (153.3)	336.5 (112.1)	102 (16)
Tundra	30.0	463.9 (118.4)	239.6 (61.4)	113 (20)

[a] Proportional area represented within the 2.2 million km^2 vegetated study domain.
[b] Mean annual GPP and NPP (standard deviations in parentheses) for the 1988–2000 period.
[c] Mean annual spring thaw date (standard deviations in parentheses) for the 1988–2000 period.

1972). The magnitude of maximum LAI in spring was directly proportional to summer and annual maximum LAI ($r = 0.685; P = 0.01$). Thus strong vegetation canopy growth in spring appears to promote greater canopy cover for the year.

The timing of the SSM/I-derived spring thaw event was inversely proportional to maximum LAI in spring ($r = -0.831; P = 0.0004$) and summer ($r = -0.688; P = 0.009$; see Figure 4). Thus years with early thawing in spring generally have
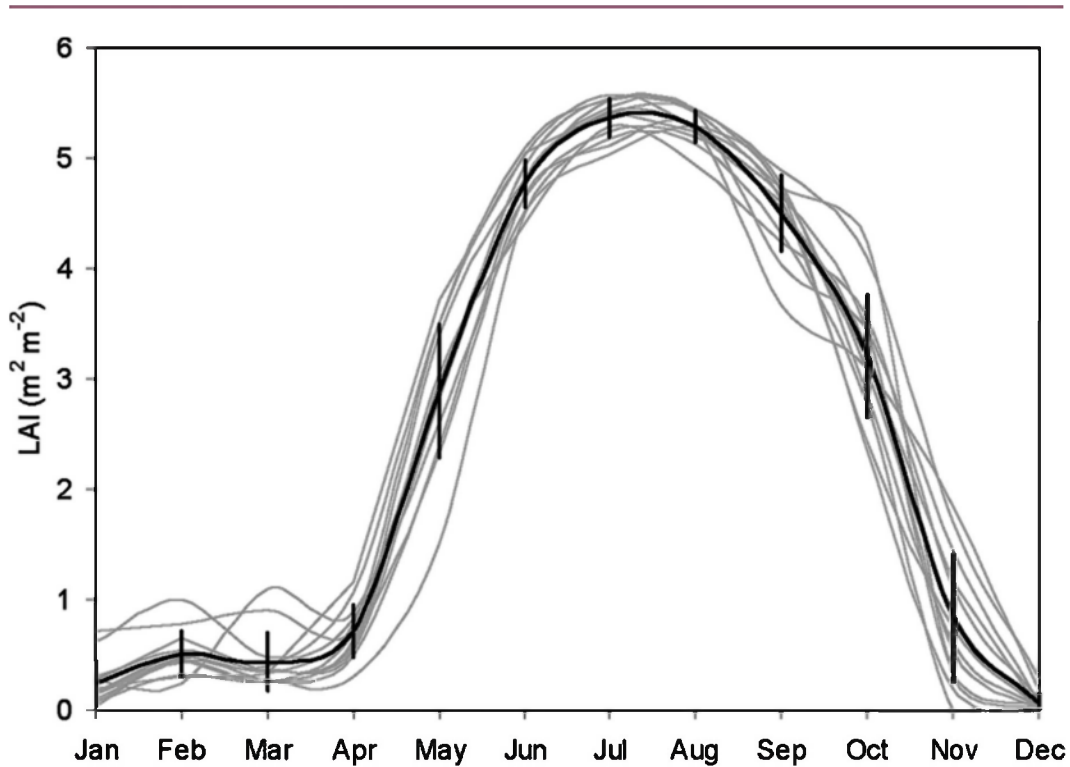
Figure 3. The seasonal cycle of mean maximum monthly LAI for the study domain as derived from the NOAA AVHRR Pathfinder record (Myneni et al. 1997a,b); the black line represents long-term (1988–2000) average conditions; vertical lines are the standard deviations of mean monthly conditions, while gray lines represent mean monthly conditions for individual years.
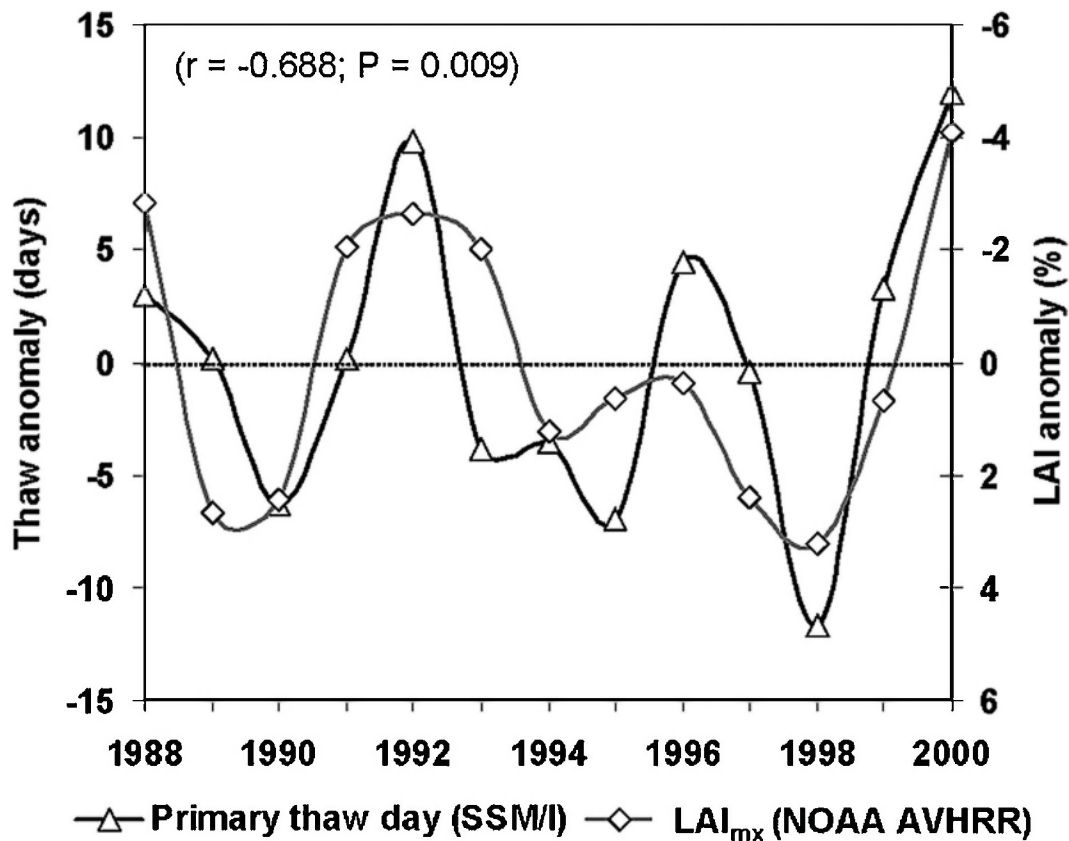
Figure 4. Annual variability and associated correspondence between SSM/I-derived timing of the primary springtime thaw event and NOAA AVHRR Pathfinder observations of maximum annual LAI (LAI_{mx}). The time series data are expressed as annual anomalies of regional averages for the entire vegetated domain, where variability in LAI_{mx} is expressed as a proportion (%) of long-term (1988–2000) average conditions; note that the sign of the LAI axis is reversed relative to the thaw axis. Annual anomalies in LAI_{mx} are inversely proportional to the timing of springtime thaw; early thaws (negative anomaly) coincide with higher LAI (positive anomaly) relative to average conditions, while delayed thaws coincide with reduced canopy cover for the year.

greater photosynthetic leaf area, while relatively late thaws coincide with reduced canopy cover. There was no evidence of a significant relationship between thaw timing and maximum LAI levels in fall, as canopy senescence is regulated by additional factors including photoperiod and plant-available moisture (Suni et al. 2003; Kimball et al. 2004). There was also no evidence of significant relationships between monthly and seasonal maximum LAI values and mean annual and seasonal air temperatures during current or previous year time periods despite evidence that current year canopy growth is influenced by environmental conditions of the previous year (Bunn et al. 2005).

3.3. GPP and NPP variability and relations with spring thaw timing

The PEM-derived GPP and NPP values for the study domain averaged 597 [±173.7 (s)] and 301 [±107.4 (s)] g C m^{-2} yr^{-1}, respectively (see Figure 5 and Table 1). Mean annual productivity within boreal forest areas was approximately 12.2% greater than regional average conditions, while arctic tundra annual productivity was 21.3% lower than the regional mean. A more detailed assessment of PEM results for the WALE domain is presented by Kimball et al. (Kimball et al. 2006), indicating that the relative magnitudes and spatial variability of the GPP and NPP values are generally consistent with other boreal and arctic productivity estimates derived from biophysical process models, in situ measurements, and stand inventory–based approaches. Within a given biome, annual productivity was generally inversely proportional to latitude and elevation, consistent with environ-
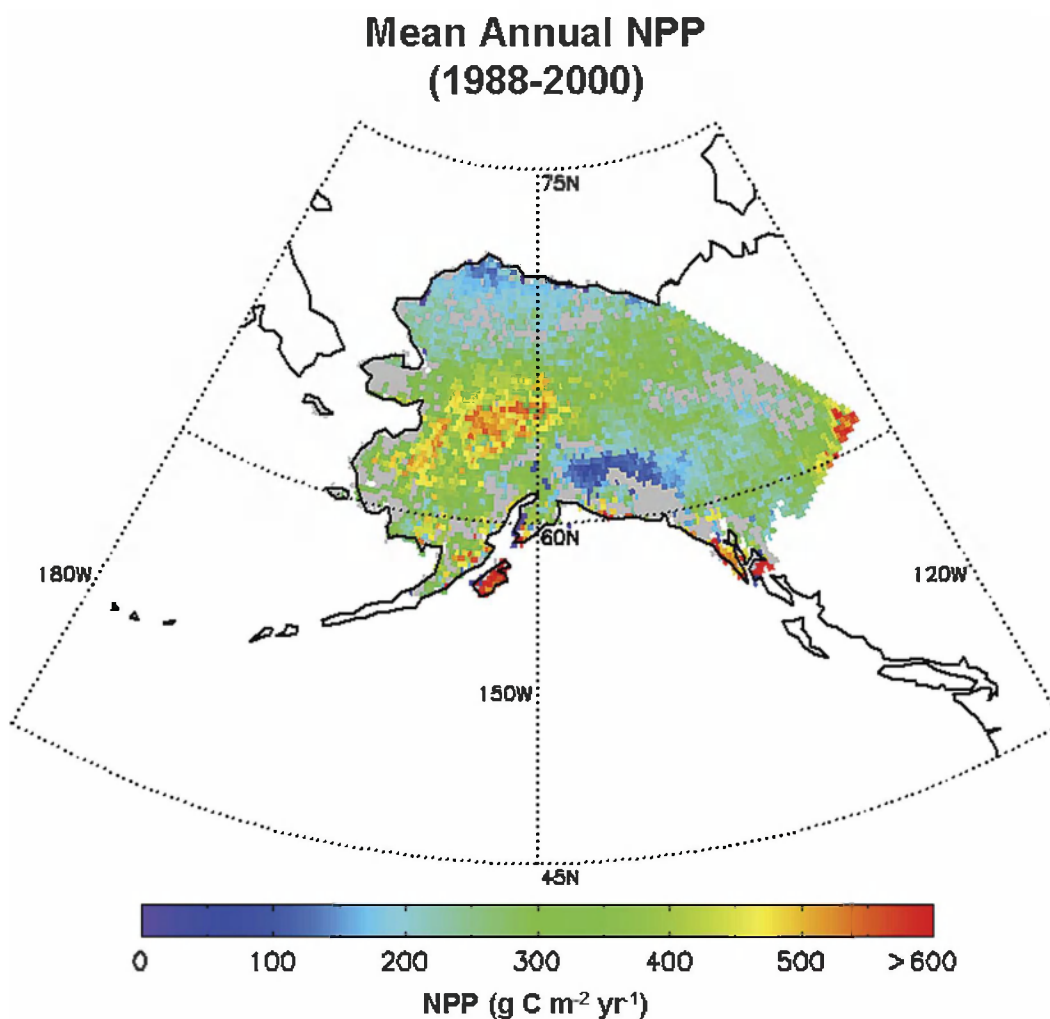

Figure 5. Mean annual NPP (g C m^{-2} yr^{-1}) derived from PEM calculations over the study domain and 13-yr (1988–2000) period; masked areas are shown in gray, while areas outside the domain are shown in white.

mental gradients in seasonal air temperatures and solar irradiance. Net primary production accounted for approximately 50% [±1.3 (s)] of GPP; there was also strong correspondence between PEM-based GPP and NPP results (r = 0.988; P < 0.0001). Similar stability in the proportion of NPP to GPP has also been reported for a range of global biomes (Waring et al. 1998; Gifford 2003), though other evidence indicates that this ratio may change over the coarse of stand development (Mäkelä and Valentine 2001) and may not be adequately represented using biophysical models based upon predominantly mature vegetation. These results indicate similar temporal behavior in both autotrophic respiration and plant photosynthetic light use efficiency for the region. These results also indicate that temperature, rather than moisture availability [as represented by the VPD parameter in Equation (2)], is the primary constraint to canopy photosynthesis and NPP for the domain and is consistent with other evidence that vegetation productivity in boreal-arctic biomes is primarily limited by low temperatures (Nemani et al. 2003).

Results of the PEM sensitivity analysis indicated that weather conditions (with constant vegetation) alone explained more than 93% (P < 0.0001) of annual GPP and NPP variability for the domain. Changes in vegetation cover (with constant climate) alone were of secondary importance, capturing approximately 80% and 70% (P < 0.0004) of GPP and NPP variability. These results are consistent with a companion analysis of vegetation productivity for the same region, indicating that a summer warming trend was primarily responsible for a positive boreal-arctic vegetation growth response from 1982 to 2000 (Kimball et al. 2006). However, these results differ from other pan-Arctic and global-scale studies indicating a greater role of vegetation cover change in driving vegetation productivity trends (Nemani et al. 2003; Goetz et al. 2005). Differences between the current results and studies involving larger spatial domains may reflect the increasing influence of additional constraints to boreal vegetation productivity and LAI including increasing water limitations to canopy growth under warmer temperature conditions, particularly for drought-sensitive southern boreal forest regions of Eurasia and North America (Nemani et al. 2003; Barber et al. 2000; Bunn et al. 2005), and the short-term, negative effects of fire-related disturbance on LAI (Hicke et al. 2003; Goetz et al. 2006).

The SSM/I-derived timing of the primary thaw event in spring was inversely proportional to AVHRR PEM–derived annual anomalies in both GPP (r = −0.851; P = 0.0002) and NPP (r = −0.857; P = 0.0001) for the study domain (see Figure 6). Years with relatively early seasonal thawing showed generally greater annual productivity, while years with delayed seasonal thawing showed reduced productivity. The slopes of these relationships also indicate that the region accumulates or loses approximately 1% of annual NPP and GPP (4 and 6 g C m^{-2}, respectively) on a daily basis depending on the timing of the springtime thaw event. These results are consistent with previous stand-level assessments of both above-ground and total NPP sensitivity to spring thaw timing for a variety of North American boreal and subalpine evergreen coniferous forests and temperate broad-leaved deciduous forests (Baldocchi et al. 2001; Kimball et al. 2000; Kimball et al. 2004).

The volcanic eruption of Mt. Pinatubo in June of 1991 has been linked with short-term (1–2 yr) cooling and reduced vegetation productivity at high latitudes
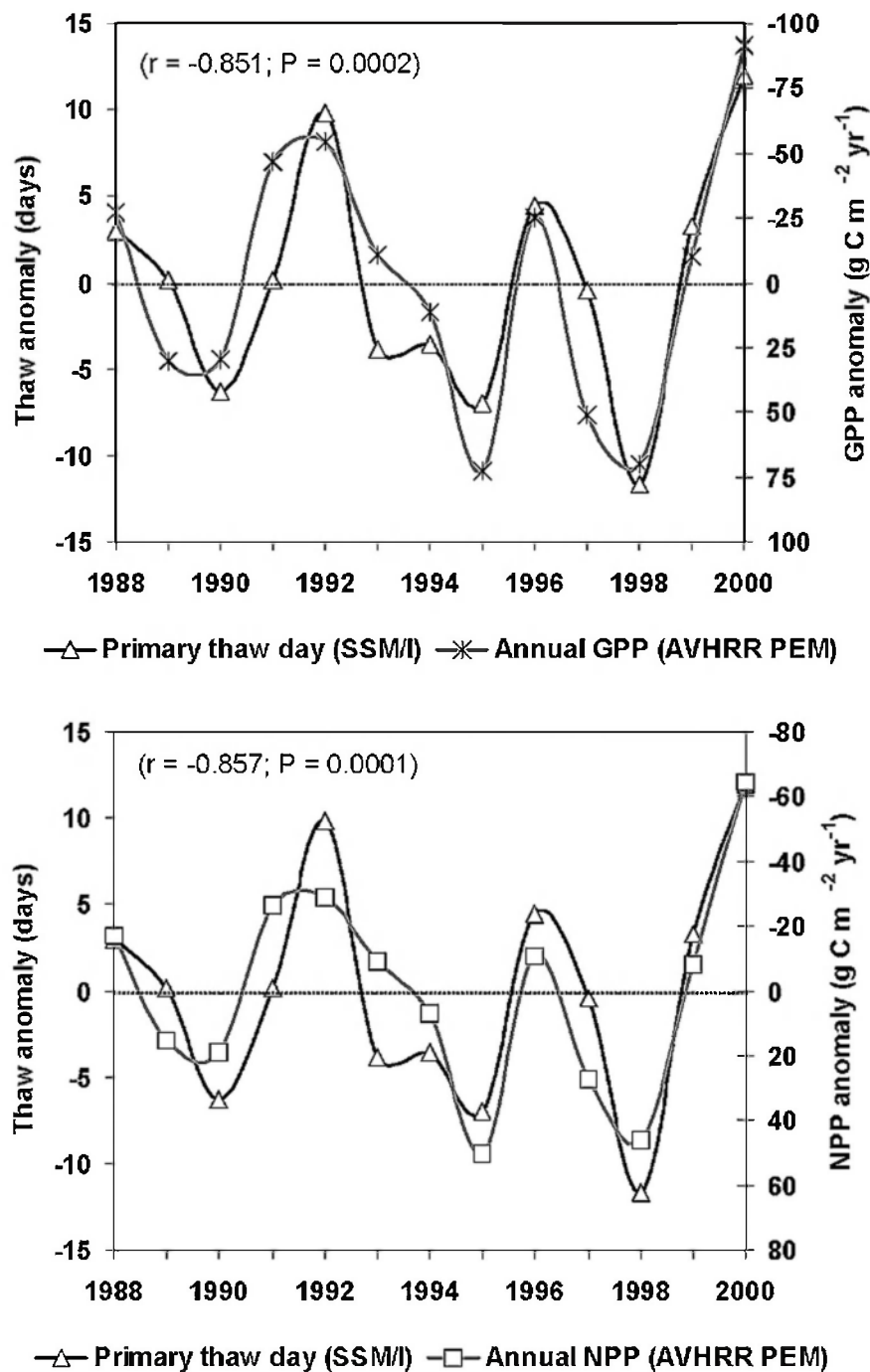
Figure 6. Annual variability and associated correspondence between SSM/I-derived springtime thaw anomalies and PEM-based (top) GPP and (bottom) NPP anomalies within the study domain; note that the sign of the GPP and NPP axes are reversed relative to the thaw axis. Annual productivity is inversely proportional to springtime thaw; early thaws (negative anomaly) coincide with greater GPP and NPP (positive anomaly) relative to average conditions, while delayed thaws coincide with decreases in annual productivity.

(Lucht et al. 2002). The average timing of the spring thaw for 1992 shows an approximate 10-day delay in the onset of the growing season relative to long-term conditions; this relative delay in growing season onset also coincided with substantial decreases (−9.2%) in annual GPP and NPP (Figure 6). Another large (12 days) delay in seasonal thawing occurred in 2000 and was the longest observed delay in the start of the growing season. The 2000 springtime thaw event also preceded anomalously cool summer air temperatures for Canada and Alaska (Houghton et al. 2001). This event coincided with 20.9% and 15.2% reductions in annual GPP and NPP, and 2000 was the least productive year of the 13-yr period. In contrast, 1995 and 1998 were the warmest and second warmest years on record for North America (Houghton et al. 2001). These two years also showed 7- and 12-day relative advances in springtime thaw and represented the earliest thaw events of the 13-yr period. The years 1995 and 1998 also showed 12% and 16% relative increases in GPP and NPP, and were the most productive years of entire study period.

4. Discussion

4.1. Physiological basis of the vegetation productivity response to spring thaw

Timing of the primary springtime thaw event, as detected by temporal classification of the satellite microwave remote sensing time series, has been found to coincide with the onset of the growing season and to be inversely proportional to the potential period of photosynthesis in boreal and subalpine evergreen coniferous forests (Frolking et al. 1999; Kimball et al. 2004). The results of this investigation indicate that an early arrival of seasonal thawing promotes greater vegetation growth and associated sequestration of atmospheric CO_2 in vegetation biomass, indicated by positive anomalies in GPP, NPP, and LAI. Alternatively, relative delays in springtime thaw promote the opposite response. These findings are consistent with stand-level studies of the relationship between springtime thaw and the seasonal shift in CO_2 exchange from a net source to sink of atmospheric carbon for boreal forests and arctic tundra (Frolking et al. 1999; Jarvis and Linder 2000; Harazono et al. 2003). These findings are also consistent with a pan-Arctic assessment of the SSM/I-derived thaw signal indicating that the timing of the primary springtime thaw event is coincident with growing season initiation and the timing and magnitude of the seasonal drawdown of atmospheric CO_2 by net photosynthesis (McDonald et al. 2004).

At high (>50°N) northern latitudes, cold temperatures and limited photoperiod largely constrain the growing season to a relatively brief period during the spring and summer months. These conditions contrast with temperate latitudes where growing seasons begin earlier and can extend well into the fall (Nemani et al. 2003). The physiological basis for this response is that low temperatures inhibit plant photosynthesis and respiration by decreasing enzyme activity and protein synthesis in plant cells (Raich and Schlesinger 1992). Low temperatures also constrain photosynthesis and canopy gas exchange by limiting water supply and mobility in roots and xylem, leading to canopy stomatal closure (Woodward and Kelly 1997). Boreal forest and tundra vegetation are well adapted to these harsh

conditions and maintain dormancy during the winter months (Havranek and Tranquillini 1995). In the spring, solar irradiance is near the seasonal maximum, and photosynthesis and NPP recover and proceed at relatively high rates following snowmelt and the new release of water in the landscape (Kimball et al. 2004; Suni et al. 2003). Photosynthesis can also occur in evergreen coniferous forests prior to this event if canopy temperatures are thawed, but vegetation growth is strongly limited by frozen soils and low moisture availability until seasonal thawing and snowmelt. Earlier onset of springtime thaw facilitates earlier and stronger net photosynthesis and annual productivity because incident solar radiation and plant-available moisture following seasonal snowmelt is relatively abundant, and autotrophic respiration is constrained by cool temperatures relative to warmer and drier conditions later in the growing season. During later stages of the growing season in the fall, potential productivity is substantially reduced by decreasing photoperiod. Thus, even if enhanced air temperatures were to extend the growing season in the fall, the net effect on annual productivity would be relatively minor compared to a similar extension in the spring. Thus year-to-year changes in the timing of growing season onset, indicated by the satellite microwave remote sensing–derived springtime thaw signal, have a significant impact on annual vegetation productivity and canopy phenology.

Surface temperature records from biophysical station networks and global climate models show a recent and unprecedented warming trend at high northern latitudes consistent with global climate change (Serreze et al. 2000; Houghton et al. 2001). Regional analyses of the annual cycles and recent trends in vegetation greenness and atmospheric CO_2 concentrations indicate a general seasonal advance and positive trend in vegetation productivity for northern latitudes that are consistent with the view that increasing air temperatures are enhancing vegetation productivity (Myneni et al. 1997a; Randerson et al. 1999; Lucht et al. 2002). Other studies, however, indicate a more variable productivity response to warming depending on plant-available moisture limitations, vegetation type, and disturbance regime (Barber et al. 2000; Wilmking et al. 2004; Goetz et al. 2005). The apparent discrepancies between these studies may reflect differences in the NPP proxies considered (e.g., above ground versus total NPP and tree ring increment versus spectral vegetation greenness index and biophysical model–based NPP), and the biophysical datasets, spatial scales, and periods of record evaluated.

In boreal and arctic environments, temperature regulates photosynthesis and canopy growth in the spring primarily through low temperature constraints on plant metabolic activity, available soil moisture, and canopy stomatal regulation of CO_2 and water vapor exchange (Jarvis et al. 2001; Suni et al. 2003; Black et al. 2000). Temperature also impacts canopy growth and LAI indirectly by regulating soil organic matter decomposition and the availability and uptake of soil nutrients (primarily N). The results of this investigation show no significant relationship between LAI and seasonal air temperatures, which may be due to one or more factors including the negative effects of temperature-induced drought stress on canopy development during warmer and drier years (Barber et al. 2000; Wilmking et al. 2004), as well as a general positive relationship between air temperature and boreal fire activity, and the potential negative impacts of fire disturbance on LAI during warmer years (Duffy et al. 2005; Hicke et al. 2003). The coarse (1.875°) spatial scale of the NCEP–NCAR reanalysis surface meteorology also does not

resolve subgrid-scale heterogeneity in surface temperature patterns and may not effectively represent potential linkages to LAI.

The satellite microwave remote sensing–derived thaw signal coincides with snowmelt and the new release of plant-available moisture in boreal-arctic landscapes, which largely initiates and sustains the recovery of photosynthetic capacity and canopy development in the spring (Jarvis and Linder 2000; Kimball et al. 2004). Thus, annual variability in the timing of thaw has a direct impact on LAI by regulating the initiation and duration of canopy photosynthesis. The results of this investigation show a relatively strong relationship between LAI and spring thaw timing and lack of correspondence with seasonal air temperatures. These findings indicate that canopy growth in spring and summer is more responsive to the timing of seasonal thawing than air temperature once thawing has occurred.

4.2. Relations between productivity and thaw trends

A satellite remote sensing and prognostic model assessment of regional productivity for the western Arctic study domain shows increasing trends in LAI, GPP, and NPP of 4% to 5% decade^{-1} from 1982 to 2000 (Kimball et al. 2006). Specific mechanisms driving this positive productivity response are uncertain but have been linked to regional warming and the relaxation of cold temperature constraints to photosynthesis, and to increased soil decomposition and associated release of plant-available nutrients. Previous analyses of the SSM/I record for the pan-Arctic show a temporal advance in springtime thaw of approximately 6 days from 1988 to 2000 (Smith et al. 2004; McDonald et al. 2004). The observed sensitivity of vegetation productivity to spring thaw timing indicates that the recent thaw advance is sufficient to account for the magnitude and direction of the positive productivity trend. These results are also consistent with a recent carbon model analysis of productivity trends for the northern terrestrial latitudes indicating recent increases in vegetation biomass in response to earlier thawing and an advancing growing season in spring (Euskirchen et al. 2006). These results also indicate that the positive productivity trend is a direct response to earlier thawing in spring, rather than increasing temperatures, which is also consistent with other studies indicating a general pattern of temperature-induced moisture stress and negative NPP responses to warming. Positive vegetation growth responses may also be reinforcing an earlier thaw cycle by altering land surface albedo and energy exchange with the atmosphere (e.g., Beringer et al. 2005; Chapin et al. 2005). However, the positive productivity response to an advancing thaw cycle may decline or reverse with continued warming, without sufficient increases in plant-available moisture to sustain additional vegetation growth (Euskirchen et al. 2006). The nature of these interactions and potential feedbacks to surface energy, water, and carbon cycle dynamics are complex and require further study.

4.3. Limitations of this investigation

For this investigation, we utilized daily meteorological inputs from the NCEP reanalysis, satellite optical-infrared remote sensing measures of vegetation parameters, and general assumptions of plant physiological responses to environmental forcings to simulate regional patterns and annual variability in GPP and NPP for

Alaska and northwest Canada. The land cover information used for this study and the resulting productivity calculations largely reflect dominant, overstory vegetation and do not explicitly account for mixed or subdominant vegetation categories within individual land cover classes. The NCEP reanalysis has been found to have significant regional and temporal differences in surface temperature and precipitation compared to other regional meteorological datasets for the WALE domain (Drobot et al. 2006); the general accuracy of these coarse-resolution data is also uncertain at high latitudes where regional monitoring networks are extremely sparse and largely confined to coastal areas and lower elevations. Satellite monitoring of high-latitude regions from optical-infrared remote sensing is also problematic due to reduced solar illumination and image degradation from frequent cloud cover, smoke, and other atmospheric aerosols, while observational trends from the long-term NOAA AVHRR record are uncertain because of issues related to navigational drift and cross-calibration of instrument series (Cihlar et al. 1998; Buermann et al. 2001). The all-weather capability and orbital characteristics of the SSM/I allow frequent daily monitoring at high latitudes, though the coarse (~25 km) spatial scale of these data does not resolve subgrid-scale variability in freeze–thaw processes, especially over complex terrain and land cover. All of these factors have the potential to adversely impact the relative accuracy of satellite-based LAI, productivity, and spring thaw calculations for the region. Despite these limitations, the results of this investigation are consistent with a growing body of evidence indicating strong sensitivity between spring thaw timing and boreal-arctic NPP, and that a recent advance in the seasonal thaw cycle is sufficient to account for the direction and magnitude of a positive trend in terrestrial vegetation productivity at high northern latitudes.

5. Conclusions

The timing of springtime thaw and associated onset of the growing season has a major impact on photosynthetic biomass and vegetation productivity in boreal and arctic biomes. Satellite microwave remote sensing–based classification of the primary springtime thaw event from the SSM/I was inversely proportional to NOAA AVHRR Pathfinder–based measurements of maximum LAI in spring and summer and PEM calculations of annual GPP and NPP. Mean annual variability in spring thaw timing was on the order of ±7 days, with corresponding impacts to annual productivity of approximately 1% day^{-1}. The results of this study imply that while surface air temperature records show a relatively consistent global warming trend since the early 1980s, vegetation growth and productivity of boreal forest and arctic tundra for the western Arctic appear to be largely benefiting from regional warming, primarily through earlier onset of the growing season. Earlier onset of springtime thaw facilitates earlier and stronger net photosynthesis and annual productivity because incident solar radiation and plant-available moisture following seasonal snowmelt is relatively abundant, and autotrophic respiration is constrained by cool temperatures relative to warmer and drier conditions later in the growing season. Vegetation productivity may also be benefiting from regional warming through increased soil organic matter decomposition and release of plant-available nutrients with thawing permafrost and warming soils (Kimball et al. 2006). While vegetation productivity may be enhanced in the short-term by an

advancing growing season, the negative effects of summer drought may become more widespread without commensurate increases in precipitation and plant-available moisture. Positive regional temperature trends have also been linked to increasing fire- and insect-related disturbances (Duffy et al. 2005). The cumulative impacts of these changes on freeze–thaw dynamics and long-term productivity are still uncertain.

References

Armstrong, R. L., and M. J. Brodzik, 1995: An Earth-gridded SSM/I data set for cryospheric studies and global change monitoring. *Adv. Space Res.,* **16,** 155–163.

——, K. W. Knowles, M. J. Brodzik, and M. A. Hardman, 2002: DMSP SSM/I Pathfinder daily EASE-Grid brightness temperatures. National Snow and Ice Data Center, Boulder, CO, digital media and CD-ROM. [Available online at http://nsidc.org/data/nsidc-0032.html.]

Baldocchi, D., and Coauthors, 2001: FLUXNET: A new tool to study the temporal and spatial variability of ecosystem-scale carbon dioxide, water vapor, and energy flux densities. *Bull. Amer. Meteor. Soc.,* **82,** 2415–2434.

Barber, V., G. P. Juday, and B. P. Finney, 2000: Reduced growth of Alaskan white spruce in the twentieth century from temperature-induced drought stress. *Nature,* **405,** 668–673.

Beringer, J., F. S. Chapin III, C. C. Thompson, and A. D. McGuire, 2005: Surface energy exchanges along a tundra-forest transition and feedbacks to climate. *Agric. For. Meteor.,* **131,** 143–161.

Black, T. A., W. J. Chen, A. G. Barr, M. A. Arain, Z. Chen, Z. Nesic, E. H. Hogg, and H. H. Neumann, 2000: Increased carbon sequestration by a boreal deciduous forest in years with a warm spring. *Geophys. Res. Lett.,* **27,** 1271–1274.

Buermann, W., J. Dong, X. Zeng, R. B. Myneni, and R. E. Dickinson, 2001: Evaluation of the utility of satellite-based vegetation leaf area index data for climate simulations. *J. Climate,* **14,** 3536–3550.

Bunn, A. G., S. J. Goetz, and G. J. Fiske, 2005: Observed and predicted responses of plant growth to climate across Canada. *Geophys. Res. Lett.,* **32,** L16710, doi:10.1029/2005GL023646.

Canny, J. F., 1986: A computational approach to edge detection. *IEEE Trans. Pattern Anal. Mach. Intell.,* **8,** 679–698.

Chapin, F. S., III, and Coauthors, 2005: Role of land surface changes in Arctic summer warming. *Science,* **310,** 657–660.

Cihlar, J., J. M. Chen, Z. Li, F. Huang, R. Latifovic, and R. Dixon, 1998: Can interannual land surface signal be discerned in composite AVHRR data? *J. Geophys. Res.,* **103D,** 23 163–23 172.

Comiso, J. C., 2003: Warming trends in the Arctic from clear sky satellite observations. *J. Climate,* **16,** 3498–3510.

DeFries, R. S., M. Hansen, J. R. G. Townshend, and R. Sohlberg, 1998: Global land cover

classifications at 8 km spatial resolution: The use of training data derived from Landsat imagery in decision tree classifiers. *Int. J. Remote Sens.,* **19,** 3141–3168.

Drobot, S., J. Maslanik, U. C. Herzfeld, C. Fowler, and W. Wu, 2006: Uncertainty in temperature and precipitation datasets over terrestrial regions of the western Arctic. *Earth Interactions,* in press.

Duffy, P. A., J. E. Walsh, J. M. Graham, D. H. Mann, and T. S. Rupp, 2005: Impacts of large-scale atmospheric-ocean variability on Alaskan fire season severity. *Ecol. Appl.,* **15,** 1317–1330.

Euskirchen, E. S., and Coauthors, 2006: Importance of recent shifts in soil thermal dynamics on growing season length, productivity, and carbon sequestration in terrestrial high-latitude ecosystems. *Global Change Biol.,* **12,** 731–750.

Frolking, S., K. C. McDonald, J. S. Kimball, J. B. Way, R. Zimmermann, and S. W. Running, 1999: Using the space-borne NASA scatterometer (NSCAT) to determine the frozen and thawed seasons of a boreal landscape. *J. Geophys. Res.,* **104,** 27 895–27 907.

Gifford, R. M., 2003: Plant respiration in productivity models: Conceptualisation, representation and issues for global terrestrial carbon-cycle research. *Funct. Plant Biol.,* **30,** 171–186.

Goetz, S. J., A. G. Bunn, G. J. Fiske, and R. A. Houghton, 2005: Satellite-observed photosynthetic trends across boreal North America associated with climate and fire disturbance. *Proc. Natl. Acad. Sci. USA,* **102,** 13 521–13 525.

——, G. J. Fiske, and A. G. Bunn, 2006: Using satellite time-series data sets to analyze fire disturbance and forest recovery across Canada. *Remote Sens. Environ.,* **101,** 352–365.

Harazono, Y., M. Mano, A. Miyata, R. C. Zulueta, and W. C. Oechel, 2003: Inter-annual carbon dioxide uptake of a wet sedge tundra ecosystem in the Arctic. *Tellus,* **55B,** 215–231.

Havranek, W. M., and W. Tranquillini, 1995: Physiological processes during winter dormancy and their ecological significance. *Ecophysiology of Coniferous Forests,* W. K. Smith and T. M. Hinckley, Eds., Academic Press, 95–124.

Heinsch, F. A., and Coauthors, cited, 2003: User's guide, GPP and NPP (MOD17A2/A3) products NASA MODIS land algorithm. [Available online at http://www.ntsg.umt.edu/modis.]

——, and Coauthors, 2006: Evaluation of remote sensing based terrestrial productivity from MODIS using regional tower eddy flux network observations. *IEEE Trans. Geosci. Remote Sens.,* **44,** 1908–1925.

Hicke, J. A., and Coauthors, 2003: Postfire response of North American boreal forest net primary productivity analyzed with satellite observations. *Global Change Biol.,* **9,** 1145–1157.

Houghton, J. T., Y. Ding, D. J. Griggs, M. Noguer, P. J. van der Linden, X. Dai, K. Maskell, and C. A. Johnson, Eds., 2001: *Climate Change 2001: The Scientific Basis.* Cambridge University Press, 881 pp.

James, M. E., and S. N. V. Kalluri, 1994: The Pathfinder AVHRR land data set: An improved coarse resolution data set for terrestrial monitoring. *Int. J. Remote Sens.,* **15,** 3347–3363.

Jarvis, P., and S. Linder, 2000: Constraints to growth of boreal forests. *Nature,* **405,** 904–905.

——, B. Saugier, and E.-D. Schulze, 2001. Productivity of boreal forests. *Terrestrial Global Productivity,* J. Roy, B. Saugier, and H. A. Mooney, Eds., Academic Press, 211–244.

Keeling, C. D., J. F. S. Chin, and T. P. Whorf, 1996: Increased activity of northern vegetation inferred from atmospheric CO_2 measurements. *Nature,* **382,** 146–149.

Kimball, J. S., A. R. Keyser, S. W. Running, and S. S. Saatchi, 2000: Regional assessment of boreal forest productivity using an ecological process model and remote sensing parameter maps. *Tree Physiol.,* **20,** 761–775.

——, K. C. McDonald, A. R. Keyser, S. Frolking, and S. W. Running, 2001: Application of the NASA Scatterometer (NSCAT) for classifying the daily frozen and non-frozen landscape of Alaska. *Remote Sens. Environ.,* **75,** 113–126.

——, ——, S. W. Running, and S. Frolking, 2004: Satellite radar remote sensing of seasonal growing seasons for boreal and subalpine evergreen forests. *Remote Sens. Environ.,* **90,** 243–258.

——, and Coauthors, 2006: Recent climate-driven increases in vegetation productivity for the

western Arctic: Evidence of an acceleration of the northern terrestrial carbon cycle. *Earth Interactions,* in press.

Kistler, R., and Coauthors, 2001: The NCEP–NCAR 50-Year Reanalysis: Monthly means CD-ROM and documentation. *Bull. Amer. Meteor. Soc.,* **82,** 247–267.

Lucht, W., and Coauthors, 2002: Climatic control of the high-latitude vegetation greening trend and Pinatubo effect. *Science,* **296,** 1687–1689.

Mäkelä, A., and H. T. Valentine, 2001: The ratio of NPP to GPP: Evidence of change over the course of stand development. *Tree Physiol.,* **21,** 1015–1030.

McDonald, K. C., J. S. Kimball, E. Njoku, R. Zimmermann, and M. Zhao, 2004: Variability in springtime thaw in the terrestrial high latitudes: Monitoring a major control on the biospheric assimilation of atmospheric CO_2 with spaceborne microwave remote sensing. *Earth Interactions,* **8**. [Available online at http://EarthInteractions.org.]

McGuire, A. D., and Coauthors, 2006: The Western Arctic Linkage Experiment: Overview and synthesis. *Earth Interactions,* in press.

Myneni, R. B., C. D. Keeling, C. J. Tucker, G. Asrar, and R. R. Nemani, 1997a: Increased plant growth in the northern high latitudes from 1981–1991. *Nature,* **386,** 698–702.

——, R. R. Nemani, and S. W. Running, 1997b: Estimation of global leaf area index and absorbed par using radiative transfer models. *IEEE Trans. Geosci. Remote Sens.,* **35,** 1380–1393.

Nemani, R. R., C. D. Keeling, H. Hashimoto, W. M. Jolly, S. C. Piper, C. J. Tucker, R. B. Myneni, and S. W. Running, 2003: Climate-driven increases in global terrestrial net primary production from 1982 to 1999. *Science,* **300,** 1560–1563.

Raich, J. W., and W. A. Schlesinger, 1992: The global carbon dioxide flux in soil respiration and its relationship to vegetation and climate. *Tellus,* **44B,** 81–99.

Randerson, J. T., C. B. Field, I. Y. Fung, and P. P. Tans, 1999: Increases in early season ecosystem uptake explain recent changes in the seasonal cycle of atmospheric CO_2 at high northern latitudes. *Geophys. Res. Lett.,* **26,** 2765–2768.

Robinson, D. A., K. F. Dewey, and R. R. Heim, 1993: Global snow cover monitoring: An update. *Bull. Amer. Meteor. Soc.,* **74,** 1689–1696.

Running, S. W., P. E. Thornton, R. Nemani, and J. M. Glassy, 2000: Global terrestrial gross and net primary productivity from the Earth Observing System. *Methods in Ecosystem Science,* O. Sala, R. Jackson, and H. Mooney, Eds., Springer-Verlag, 44–57.

——, R. R. Nemani, F. A. Heinsch, M. Zhao, M. Reeves, and H. Hashimoto, 2004: A continuous satellite-derived measure of global terrestrial primary production. *Bioscience,* **54,** 547–560.

Serreze, M. C., and Coauthors, 2000: Observational evidence of recent change in the northern high latitude environment. *Climate Change,* **46,** 159–207.

——, D. H. Bromwich, M. P. Clark, A. J. Ertringer, T. Zhang, and R. Lammers, 2002: Large-scale hydro-climatology of the terrestrial Arctic drainage system. *J. Geophys. Res.,* **107,** 8160, doi:10.1029/2001JD000919.

Smith, N. V., S. S. Saatchi, and J. T. Randerson, 2004: Trends in northern latitude soil freeze and thaw cycles from 1988 to 2002. *J. Geophys. Res.,* **109,** D12101, doi:10.1029/2003JD004472.

Suni, T., F. Berninger, T. Markkanen, P. Keronen, Ü. Rannik, and T. Vesala, 2003: Interannual variability and timing of growing-season CO_2 exchange in a boreal forest. *J. Geophys. Res.,* **108,** 4265, doi:10.1029/2002JD002381.

Ulaby, F. T., R. K. Moore, and A. K. Fung, 1986: *Microwave Remote Sensing: Active and Passive.* Vol. 1, Artec House, 456 pp.

Viereck, L. A., and E. L. Little Jr., 1972: *Alaska Trees and Shrubs.* USDA Handbook No. 410, 264 pp.

Waring, R. H., J. J. Landsberg, and M. Williams, 1998: Net primary production of forests: A constant fraction of gross primary production? *Tree Physiol.,* **18,** 129–134.

Wilmking, M., G. P. Juday, V. A. Barber, and H. S. J. Zald, 2004: Recent climate warming forces contrasting growth responses of white spruce at treeline in Alaska through temperature thresholds. *Global Change Biol.,* **10,** 1724–1736.

Woodward, F. I., and C. K. Kelly, 1997: Plant functional types: Towards a definition by environmental constraints. *Plant Functional Types: Their Relevance to Ecosystem Properties and Global Change*, T. M. Smith, H. H. Shugart, and F. I. Woodward, Eds., Cambridge University Press, 47–65.

Zhao, M., F. A. Heinsch, R. R. Nemani, and S. W. Running, 2005: Improvements of the MODIS terrestrial gross and net primary production global dataset. *Remote Sens. Environ.*, **95,** 164–176.